Supplementary material for

Distal chromatin structure influences local nucleosome positions and gene expression

An Jansen[1,2], Elisa van der Zande[1,2], Wim Meert[1,2], Gerald R. Fink[3]* and Kevin J. Verstrepen[1,2]*

[1]Laboratory for Systems Biology, VIB, Bio-Incubator, Gaston Geenslaan 1, B-3001 Leuven, Belgium
[2]Laboratory for Genetics and Genomics, Centre of Microbial and Plant Genetics (CMPG), K.U.Leuven, Kasteelpark Arenberg 22, B-3001 Leuven, Belgium
[3]Whitehead Institute for Biomedical Research/M.I.T., Nine Cambridge Center, Cambridge, MA 02142, USA

*Correspondence:

Kevin.Verstrepen@biw.vib-kuleuven.be
Ph: +32 (0)16 751393

GFink@wi.mit.edu
Ph: +1 617 258 5215

Supplementary materials and methods

Yeast strains. Strains, plasmids and primers used in this study are listed in Tables SI, SII and SIII respectively. Yeast strains used in this study are derived from S288C strain BY4741 (41). This strain does not have a copy of the *URA3* gene. To generate a *URA3*+ strain, we integrated the *URA3* gene at the native *URA3* locus. Primers KV2478 and KV2479 were used to amplify *URA3* from FY4 genomic DNA, and the PCR product was transformed into BY4741, creating strain AJY248.

Progressive deletions of the *URA3* promoter at the native *URA3* locus. Standard procedures for isolation and manipulation of the DNA were used (47-49). Takara ExTaq DNA polymerase was used for the amplification of DNA fragments by PCR. The primers used for the PCR amplification were obtained from IDT (Coralville, IA and Leuven, Belgium). Standard DNA sequencing for confirming partial *URA3* promoter deletions and point mutations was carried out by the VIB Genetic Service Facility, Antwerp, Belgium.

Two strategies were employed to construct *URA3* promoter mutants at the native *URA3* locus. The first strategy is based on the "delitto perfetto" approach for *in vivo* site-directed mutagenesis using oligonucleotides (50). The *LYS2* gene in strain AJY248 was deleted by integrative transformation, using *K. lactis LEU2* from pUG73 as selection marker and primers KV2613 and KV2614 for amplification of DNA fragments by PCR (AJY536). Next, the counter-selectable *LYS2* marker was amplified from BY4741 genomic DNA using primers KV2617 and KV2618 and integrated by transformation into the *URA3* promoter of this strain, creating AJY543. For each *URA3* promoter mutant, two 90-nucleotide integrative recombinant oligonucleotides (IROs) were designed with a 10-base overlap at their 3' ends. They were annealed and extended with Pfx DNA polymerase (Platinum Pfx DNA Polymerase, Invitrogen), resulting in a 170 bp double stranded molecule that contains 80 bp homologous with sequence upstream of and 80 bp downstream from the *LYS2* marker. Strain AJY543 was transformed with these molecules, deleting the *LYS2* marker and sufficient surrounding sequences to create the required *URA3* promoter deletion. Transformants were selected on α-aminoadipic acid (α-AA) medium which allows for selection of *lys2* and *lys5* mutants (51,52). However, this method generated a large number of false-positive clones in each transformation, presumably due to (spontaneous) mutations in the *LYS2* or *LYS5* genes resulting in non-functional alleles that would allow the isolate to grow on α-AA medium.

For that reason, another strategy was developed. In strain AJY248, the *URA3* gene was deleted by integrative transformation and replaced by the *LYS2* marker, which was amplified from BY4741 genomic DNA using primers KV2619 and KV2620 (AJY545). The *URA3* gene was amplified from pRS306 or AJY248 genomic DNA, using reverse primer KV3024 and various different forward primers generating *URA3* constructs with different promoter lengths. These constructs were integrated by transformation into the native *URA3* locus of strain AJY545, replacing the *LYS2* marker. Transformants were selected on α-AA medium. Using this method, a very low number of checked isolates were false-positive.

Integrating the *URA3* gene and altering the *URA3* promoter sequence at various genomic locations. The *URA3* gene was integrated at various genomic locations by transforming DNA fragments amplified from pRS306 or FY4 genomic DNA into BY4741. *URA3* promoters of varying lengths were created by using forward primers homologous to different regions of the promoter. In addition to the partial 5' deletion of their *URA3* promoter, a number of strains contain (a) point mutation(s) in the remaining promoter sequence. Point mutations were introduced simultaneously with the partial deletion by using forward primers that contain the desired sequence change. Transformants were selected on α-AA medium.

Deletion of the poly(dA:dT) sequence in the *URA3* promoter. The poly(dA:dT) tract of the *URA3* promoter has been defined as the T-rich sequence between -206 and -157 bp relative to the ATG (27). We used primers AJ167 and AJ168 to PCR amplify *URA3* without the poly(dA:dT) sequence from FY4 genomic DNA. This was achieved by designing primer AJ167 to contain sequence homologous to the DNA upstream (78 bp) and downstream (22 bp) of the poly(dA:dT) stretch, but not to the poly(dA:dT) stretch itself. The amplified DNA fragment was subsequently transformed into strain FY4 *URA3*::*KanMX6*, and Ura+ transformants were selected and sequenced. Genomic DNA of isolates lacking the poly(dA:dT) sequence in the *URA3* promoter was used as a template for PCR amplification of the *URA3* gene, and the PCR product was transformed into BY4741 to obtain strains AJY246 and AJY250 (using primers KV2478 × KV2479 and AJ149 × KV2433 respectively).

Fluorescent tagging of *URA3*. The *URA3* protein was tagged with yellow fluorescent protein (YFP) variant yECitrine (53). Primers KV2809 and KV2916 were used to PCR amplify yECitrine and the *SpHIS5* or *Kan* selectable markers from plasmids pKT139 or pKT140 respectively. The PCR products were transformed into multiple strains carrying the *URA3* gene. Transformants were selected on either SC-his medium (pKT139) or G418 medium (pKT140).

Deletion and substitution of the *LYS2* promoter. Primers AJ409 and AJ293 were used to PCR amplify the *LEU2* cassette from plasmid pRS305, and the PCR product was transformed into AJY377 to delete the *LYS2* promoter (p*LYS2*). Transformants were screened on SC-leu medium.

Media. Standard yeast media were prepared as described (42). YPD medium contained 2% glucose (Merck), 2% peptone (BD Biosciences), and 1% yeast extract (Lab M). G418 medium is YPD medium supplemented with 200 µg/ml geneticin (Invitrogen). Synthetic Complete (SC) medium contained 0.67% yeast nitrogen base without amino acids and with ammonium sulphate (BD Biosciences), 2% glucose, 0.08% CSM-URA (Dropout mix without uracil; MP Biomedicals), and 0.005% uracil (Sigma-Aldrich). 5-FOA medium is SC medium supplemented with 0.1% 5'-fluoroorotic acid (MP Biomedicals). SC-ura, SC-leu, SC-his and SC-lys media contained 0.67% yeast nitrogen base without amino acids and with ammonium sulphate, 2% glucose, and 0.08% of the appropriate drop-out mix (CSM-URA, CSM-LEU, CSM-HIS and CSM-LYS respectively; MP Biomedicals). Plates contained in addition 2%

agar (Invitrogen). α-AA plates contained 0.16% yeast nitrogen base without amino acids and without ammonium sulphate (BD Biosciences), 2% glucose, 2% agar, 0.2% α-aminoadipic acid (Sigma-Aldrich), 0.003% lysine (Sigma-Aldrich), 0.02% uracil, 0.05% histidine (Sigma-Aldrich), 0.22% leucine (Sigma-Aldrich), and 0.03% methionine (Sigma-Aldrich) (49).

Bioinformatics. Nucleosome position predictions by genomic sequence were performed online using the related Kaplan *et. al.* (2009) and Field *et. al.* (2008) models, both developed by the Segal lab (http://genie.weizmann.ac.il/software/nucleo_prediction.html; (15,21). Predictions were made using default parameters (for the Kaplan *et al.* model, nucleosome concentration = 0.1 and (inverse) temperature = 1; for the Field *et al.* model, nucleosome concentration = 1 and (inverse) temperature = 0.5). The *URA3* promoter sequence was analyzed including at least 5,000 bp of sequence upstream and downstream of the *URA3* promoter region. Data was viewed with the Genomica software (developed by Y. Lubling and E. Segal, http://genomica.weizmann.ac.il/).

Northern blot analysis. For Northern blot analysis, samples were collected as described above for quantitative PCR. Isolation and quantification of total RNA was performed as described previously (49,54). RNAs were separated on formaldehyde-agarose denaturing gels and blotted as described (55). Hybond membranes were hybridized with ^{32}P-labeled RNA probes generated with the T7 MAXIscript Kit (Ambion). Probes were generated using primers AJ448 × AJ449 (*URA3* probe), AJ450 × AJ451 (*LYS2* probe) and AJ454 × AJ455 (*TPI1* probe).

Exploration of transcription factor binding sites that potentially influence promoter nucleosome positions

The *lys2::URA3* mutant strains described have only minor differences in their *URA3* promoter sequence, yet these differences give rise to dramatically different nucleosome patterns. For example, at the 721 locus, the *URA3* promoter in mutant 163 contains well-positioned nucleosomes, whereas the nucleosome pattern of the *URA3* promoter in mutant 162 is fuzzy, yet the *URA3* promoter in these strains differs by only one nucleotide. Minor differences in the promoter sequence might create or destroy a TF binding site, or small sequence changes in a binding site might alter the affinity of a TF for its binding site. Altered TF binding can affect the nucleosome structure of the *URA3* promoter and change *URA3* expression. No known TF binding sites are located in this region of the intensively studied URA3 promoter. However, the UniPROBE database (56-58) indicates that different putative binding sites are formed at the junction between *LYS2* and the truncated *URA3* promoter in the 162 and 163 mutants (Table SVIII). Whereas strain 163 has three putative TF binding sites for Sfp1, strain 162 has only 1. In addition, the putative TF binding site for Sum1 is present in strain 163 but not in strain 162 (Table SVIII).

To investigate if a difference in TF binding sites may (partially) explain the difference in *URA3* expression in strains 162 and 163, we constructed point mutants of strains 163 and 162, destroying putative TF binding sites as well as creating novel ones (as predicted by the UniPROBE database; Table SVIII). As a result, we created a series of strains containing minor sequence differences, yet containing different putative TF binding sites in their *URA3* promoter. We characterized these strains in terms of growth and *URA3* expression (Fig. S11). All point mutants show the same growth characteristics as their parent strains (Fig. S11A,B). In addition, for strain 162 and its point mutant, *URA3* expression is similar both in YPD and SC-ura media (Fig. S11C). This is not the case for *URA3* expression in strain 163 and its derived mutants where we observe a significant decrease in *URA3* expression in the point mutants when compared to the parent strain 163 (Fig. S11C). However, expression in the point mutants of strain 163 remains significantly higher than expression in strain 162. Next, we examined the nucleosome positions of the *URA3* promoter in the mutated *lys2::URA3* strains (Fig. S12, Table SVI). Strain 163 and the mutants derived from this strain all show well-positioned nucleosomes in the *URA3* promoter. Strain 162-AA shows the same nucleosome profile as strain 162, characterized by the absence of a well-positioned +1 nucleosome. The nucleosome positions in all the strains correlate with the growth and expression data collected for these strains. In the presence of a well-positioned +1 nucleosome, both basal and induced *URA3* expression are higher than when this nucleosome is absent. In addition, strains with a well-positioned +1 nucleosome are not able to grow on 5-FOA medium and grow just as well in SC-ura medium as in YPD. When the promoter region lacks well-positioned nucleosomes, strains are able to grow on 5-FOA medium and show slower growth in SC-ura medium compared to growth in YPD.

We do not observe a correlation between the presence or absence of putative TF binding sites, and nucleosome positioning (Fig. S12, Table SVI, SVIII). For example, strains 163-A, 163-C and 162-AA all lack (functional) putative TF binding sites at the junction between *LYS2* and *URA3*, yet the nucleosome profiles of the *URA3* promoter are different. On the other hand, strains 163 and 163-G do show putative TF binding sites, but the *URA3* promoter shows the same nucleosome profile as in strains 163-A and 163-C. Together, these data indicate that differences in TF binding sites are unlikely to be the cause of the differences in URA3 expression between strains 162 and 163.

Supplementary figures

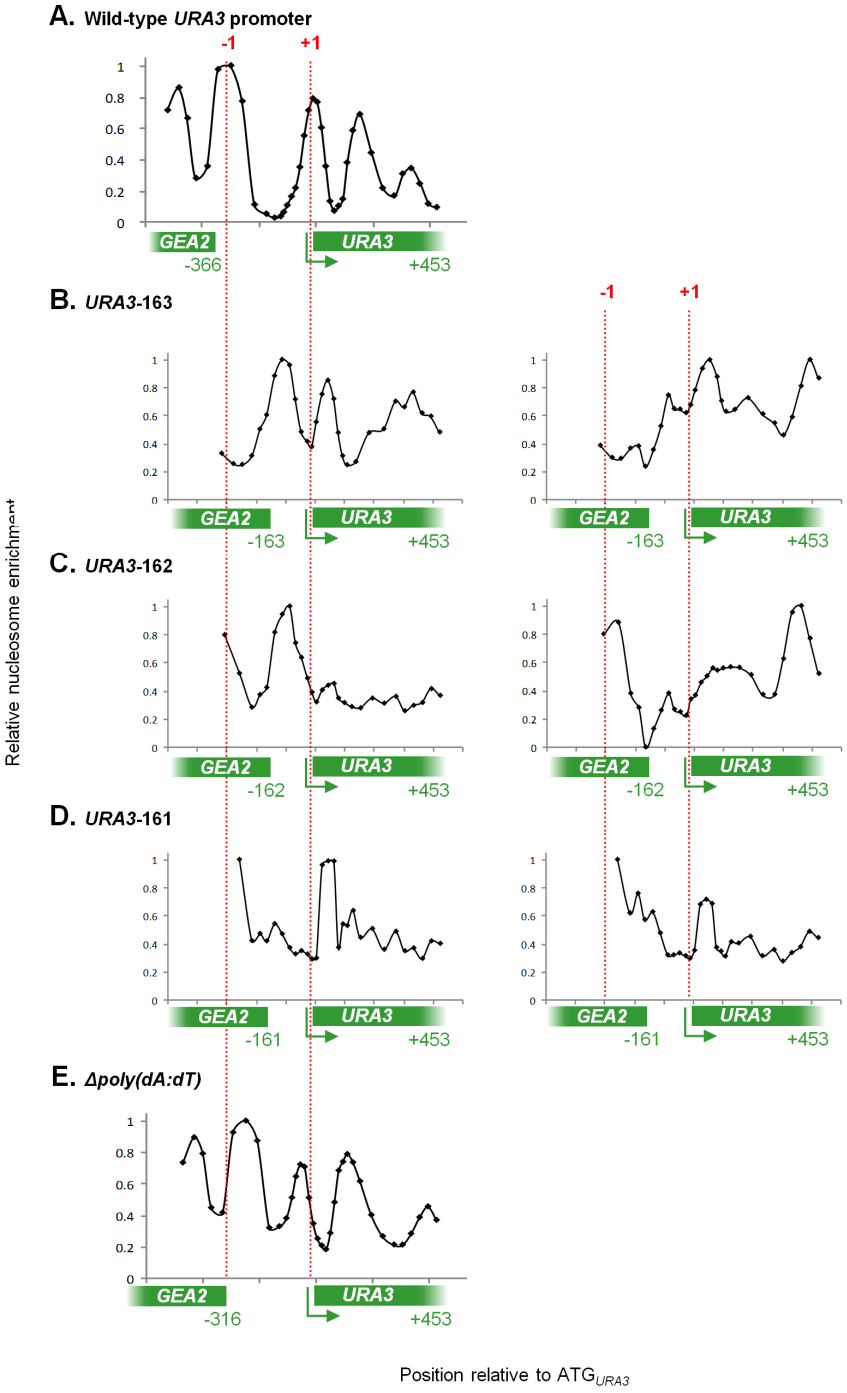

Figure S1. Nucleosome positions of the native *URA3* promoter and selected promoter mutants. Using tiling qPCR, we determined the nucleosome positions of (**A**) the wild-type *URA3* promoter at its native locus (same as Fig. 2A). In addition, we determined the nucleosome profile of selected promoter mutants, i.e. mutants (**B**) 163, (**C**) 162, (**D**) 161, and (**E**) Δ*poly(dA:dT)*. For mutants 163, 162 and 161, nucleosome positions were not reproducible between independent experiments, as illustrated by two representative nucleosome plots in panels B, C and D. Peak positions corresponding to nucleosome positions were measured (Table I). Red dotted lines mark the positions of the -1 and +1 nucleosomes in the wild-type *URA3* promoter at its native locus.

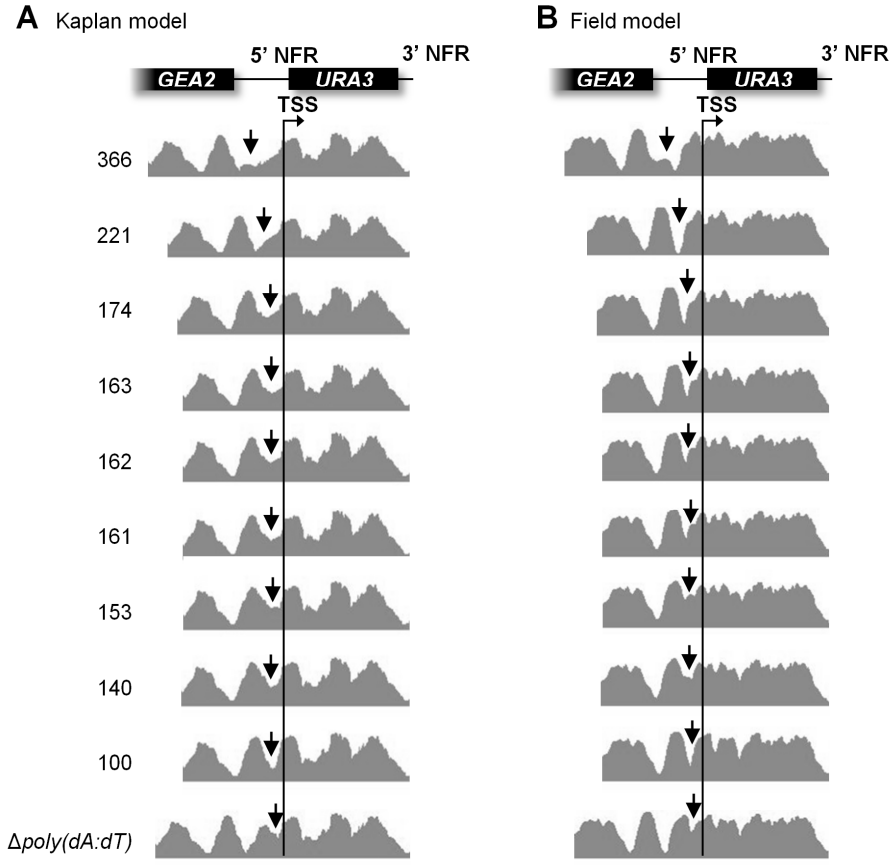

Figure S2. The predicted nucleosome positions of the native *URA3* promoter and selected promoter mutants using (**A**) the Kaplan *et. al.* model (21) and (**B**) the Field *et. al.* model (15). Arrows indicate the 5' NFR.

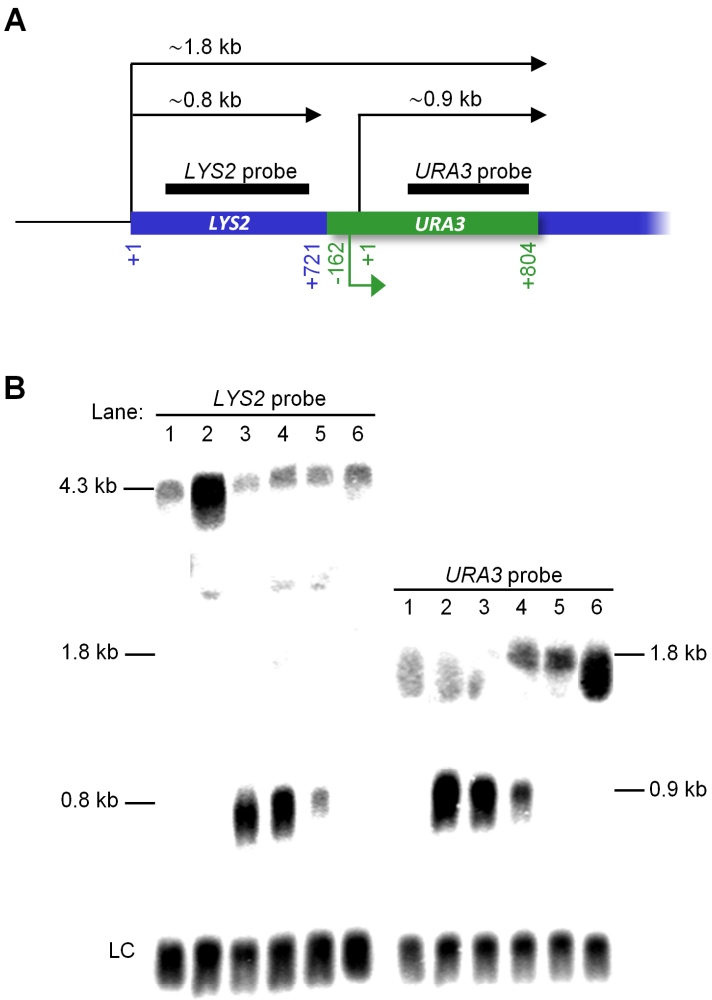

Figure S3. *LYS2* transcription does not affect *URA3* expression and the nucleosome profile of the *URA3* promoter. We relocated the *URA3* gene to the *LYS2* ORF, thereby creating *lys2::URA3* mutant strains. Although a functional Lys2 protein is no longer formed, transcription originating form the *LYS2* promoter is still taking place. Therefore, we cannot exclude that *LYS2* transcription interferes with *URA3* expression and the nucleosome structure of the *URA3* promoter. We examined the transcripts originating from the *LYS2* and *URA3* promoters under non-inducing conditions in strains 366, 163 and 162 where *URA3* is

integrated at the 721 locus. (**A**) Map of transcripts detected from mutant 162. (**B**) Northern blot analysis performed on total RNA from BY4742 (*lys2 ura3*; lane 1), AJY248 (*LYS2 URA3*; lane 2), mutant 366 (lane 3), mutant 163 (lane 4), mutant 162 (lane 5) and mutant 162 ΔP_{LYS2} (lane 6). Load control (LC) is *TPI1*. In all of these strains, a short transcript (~0.8 kb) is detected by the *LYS2* probe, indicating that *LYS2* transcription is halted where the *LYS2* gene is fused to the *URA3* promoter. However, in strains 163 and 162, a second transcript (~1.8 kb) is detected by the *LYS2* probe. This transcript is also detected by the *URA3* probe and indicates the formation of a "fusion" transcript, which would be formed if *LYS2* transcription is not halted at the *URA3* promoter but instead at the 3'UTR of the *URA3* gene. Although this transcript is only present in small amounts, it indicates that read-through transcription originating from the *LYS2* promoter does occur and the possibility exists that this interferes with *URA3* expression in strains 163 and 162. *URA3* transcription gives rises to a ~0.9 kb transcript, detected by the *URA3* probe. As expected, we observe the most *URA3* transcript being formed in strain 366 whereas in strain 162, *URA3* transcription can hardly be detected by Northern blotting. To exclude the possibility that read-through transcription in strain 162 affects *URA3* expression, we created strain 162 ΔP_{LYS2} in which the *LYS2* promoter is deleted. In this strain, no *LYS2* transcription can be detected. (**C**) Growth on solid YPD, SC-ura and 5-FOA media of strains 162 and 162 ΔP_{LYS2}. Strain 162 ΔP_{LYS2} shows the same growth phenotype on solid inducing and non-inducing media as strain 162. The nucleosome profile of the *URA3* promoters in both strains is similar (Table SVI). Thus, *LYS2* transcription has no effect on *URA3* expression nor on the positions of the *URA3* promoter nucleosomes in our *lys2::URA3* strains.

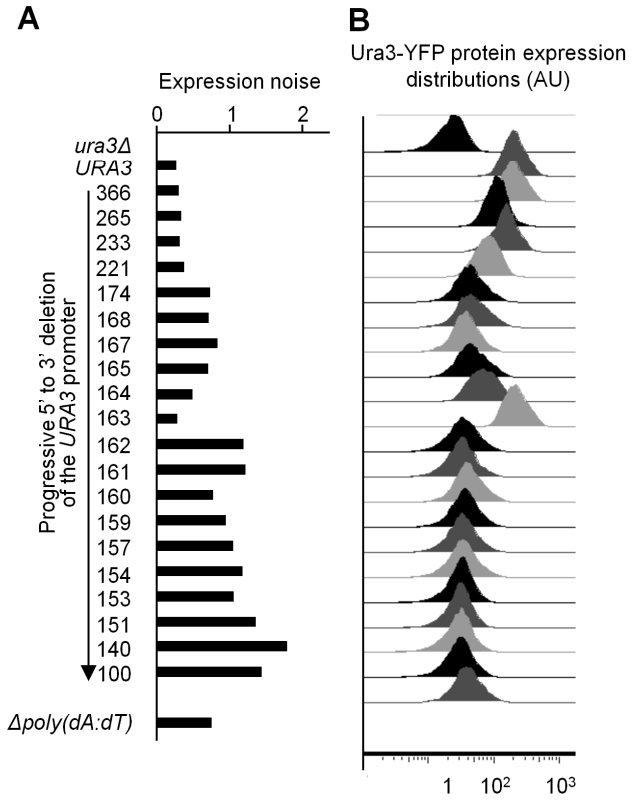

Figure S4. Expression noise in the *lys2::URA3* promoter mutants. The truncated *URA3* constructs were inserted into the *LYS2* gene, 721 bp downstream of the *LYS2* translational start site (ATG) (see also Fig. 3). 5' to 3' progressive deletion mutants are labeled by the number of remaining nucleotides in the *URA3* promoter. (**A**) Expression noise is defined as the standard deviation divided by the mean, conveying the magnitude of variability as a percentage of the level of gene expression. We observe an increase in noise that correlates with decreasing promoter length and decreasing Ura3 protein levels (Fig. 3C). However, (**B**) shows that the distribution of Ura3-YFP protein expression does not alter significantly (i.e. the standard deviation remains constant), thus indicating that the observed differences in noise can be attributed to the altered mean expression levels.

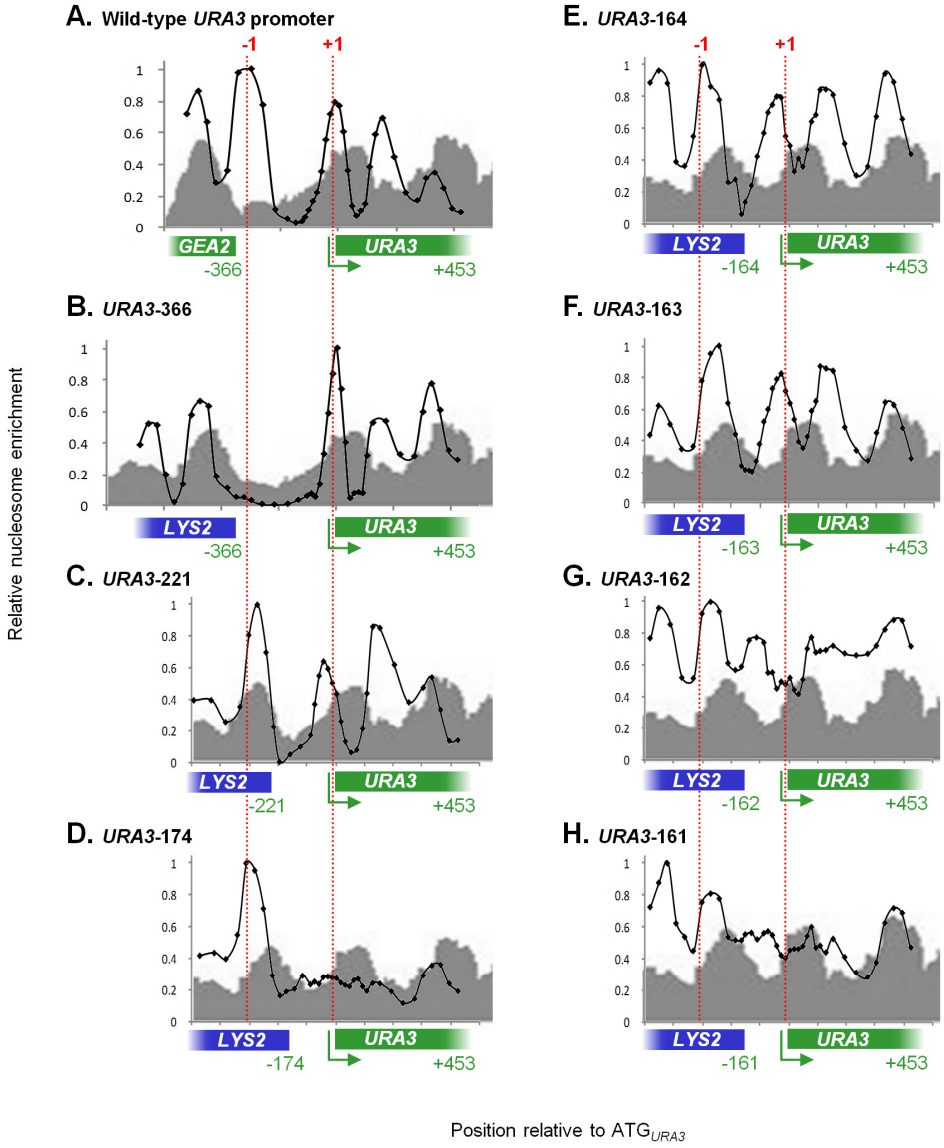

Figure S5. (figure legend on page S12)

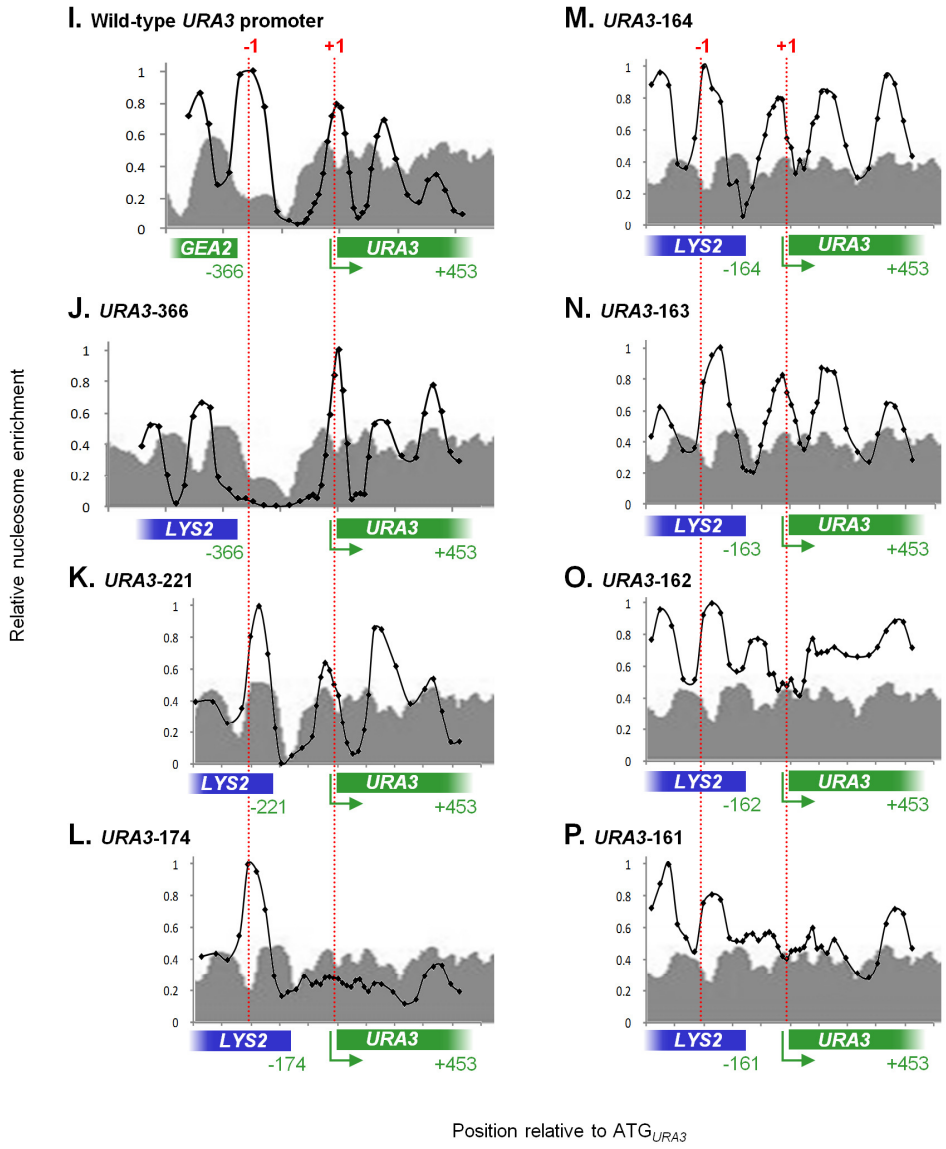

Figure S5 (continued from page S11). The experimentally determined nucleosome positions of the native *URA3* promoter and selected promoter mutants after insertion of the truncated *URA3* constructs into the *LYS2* gene, 721 bp downstream of the *LYS2* translational start site (ATG) (Fig. 4) are superimposed to the predicted nucleosome positions using the Kaplan *et al.* (A-H) (21) and Field *et. al.* models (I-P) (15). Red dotted lines mark the positions of the -1 and +1 nucleosomes in the wild-type *URA3* promoter at its native locus.

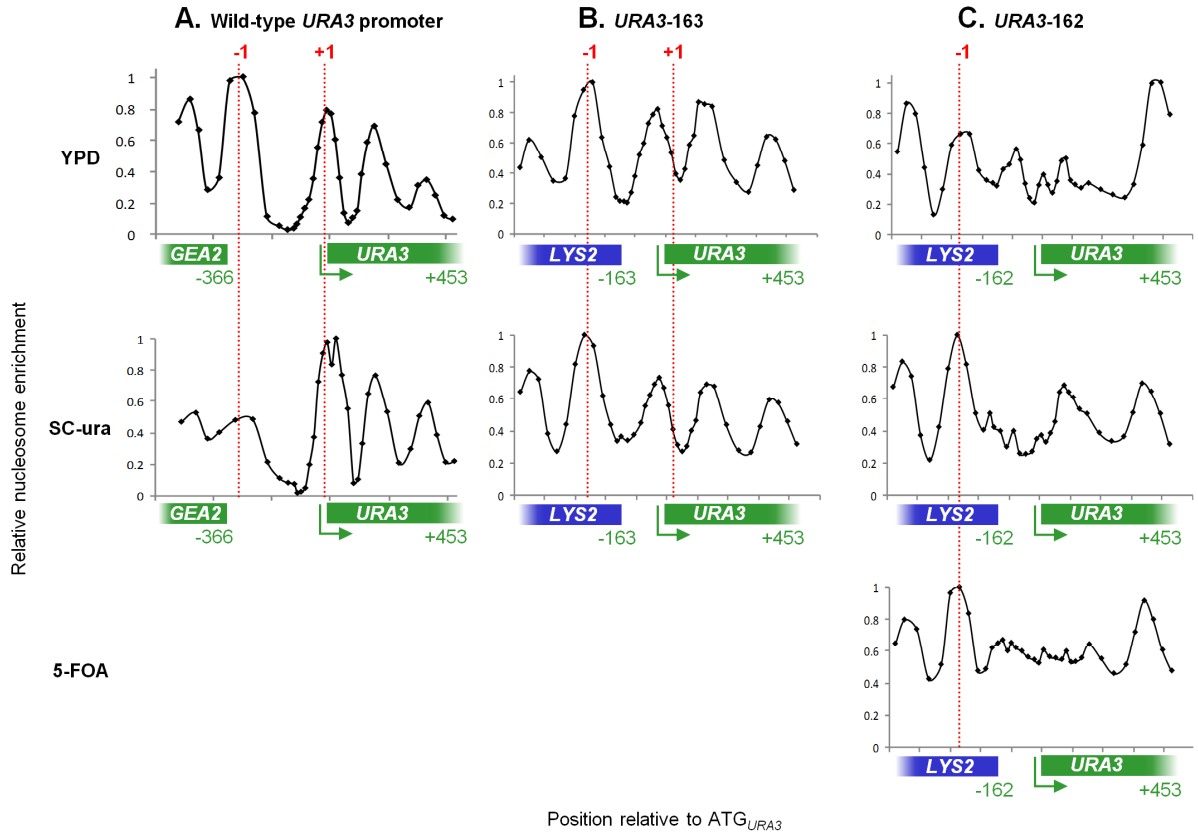

Figure S6. Promoter nucleosome positions are independent of *URA3* induction. Using tiling qPCR, we determined the nucleosome positions of (**A**) the wild-type *URA3* promoter at its native locus (same as Fig. 2A), (**B**) strain *URA3*-163 (same as Fig. 4I), and (**C**) strain *URA3*-162 (same as Fig. 4J) under inducing (SC-ura) and non-inducing (YPD, 5-FOA) conditions. Peak positions corresponding to nucleosome positions were measured (Table SVII). Red dotted lines mark the positions of the -1 and +1 nucleosomes in the wild-type *URA3* promoter at its native locus.

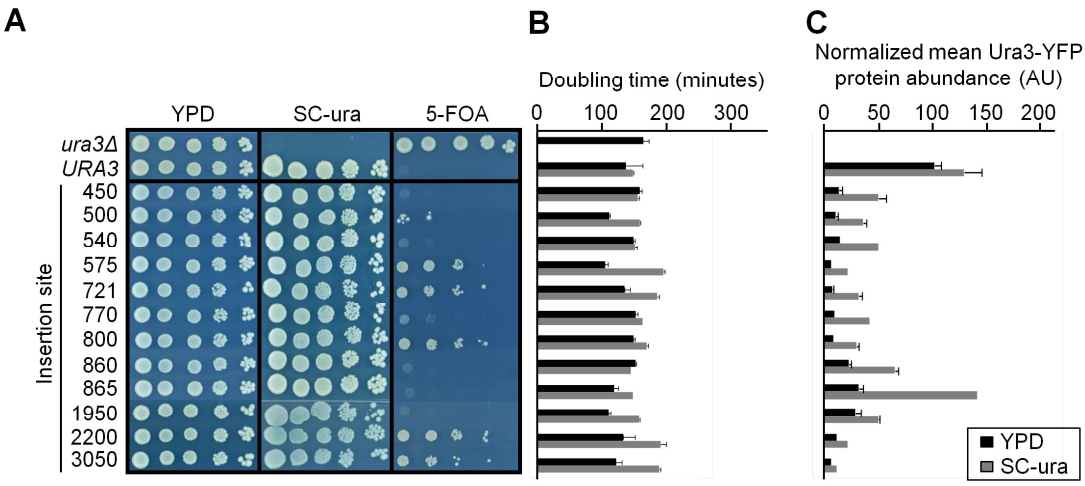

Figure S7. Expression of a truncated *URA3* gene depends on the genomic context. A truncated *URA3* construct in which 162 nt of the *URA3* promoter remain (*URA3*-162), was inserted at various locations in the *LYS2* gene (Fig. 4A). (**A**) Different insertion sites lead to different growth patterns on SC-ura and 5-FOA medium. Mutants are labeled by their location inside the *LYS2* ORF. These mutants also show differences in doubling times (**B**), and normalized mean Ura3-YFP protein abundance (**C**) for growth in liquid YPD (black bars) and liquid SC-ura (grey bars) media. Error bars denote standard deviation.

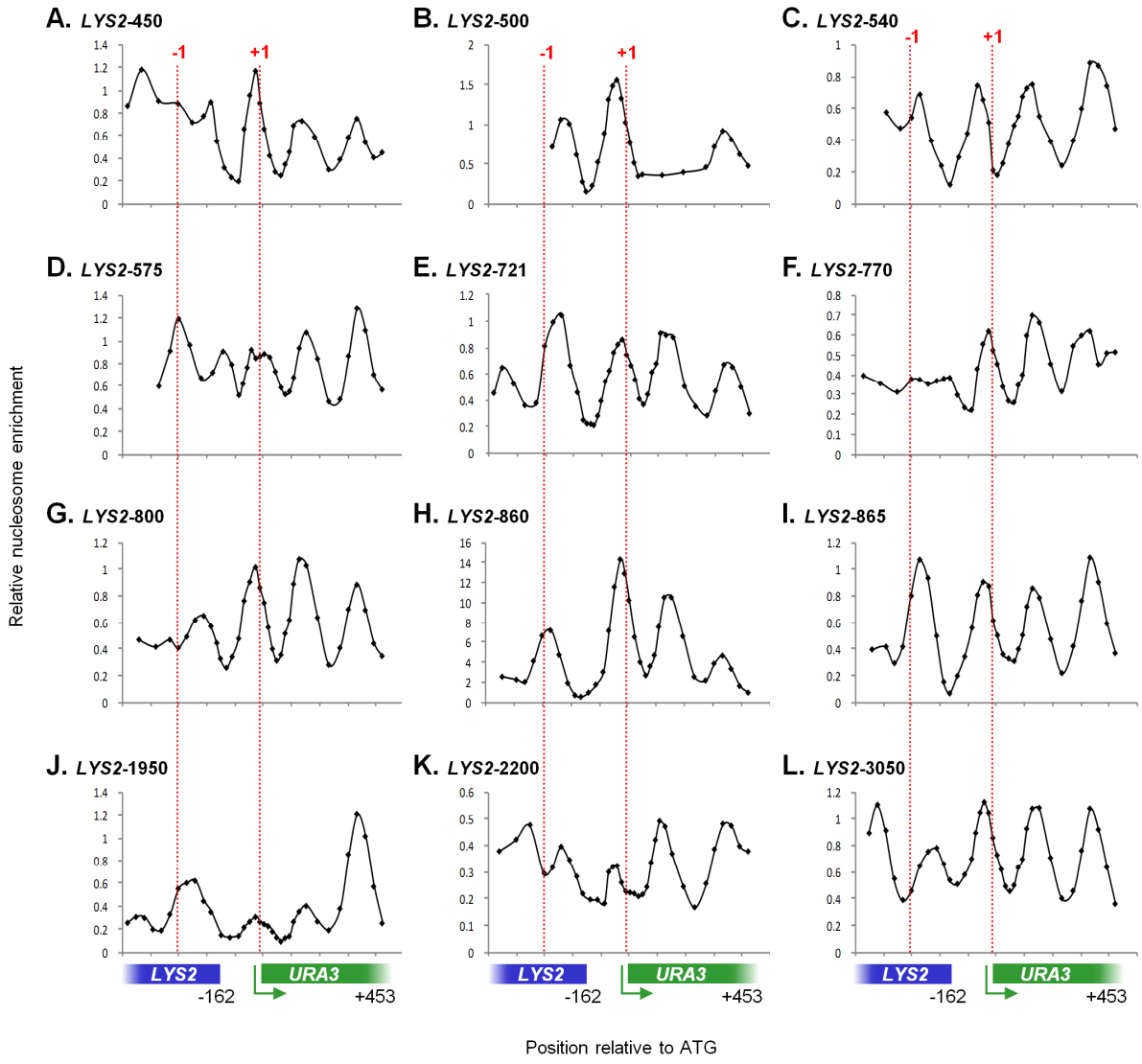

Figure S8. Nucleosome positions are influenced by the genomic context. Using tiling qPCR, we determined the nucleosome positions of the *URA3*-163 construct inserted at different positions in the *LYS2* gene. Peak positions corresponding to nucleosome positions were measured (Table I). Red dotted lines mark the positions of the -1 and +1 nucleosomes in the wild-type *URA3* promoter at its native locus.

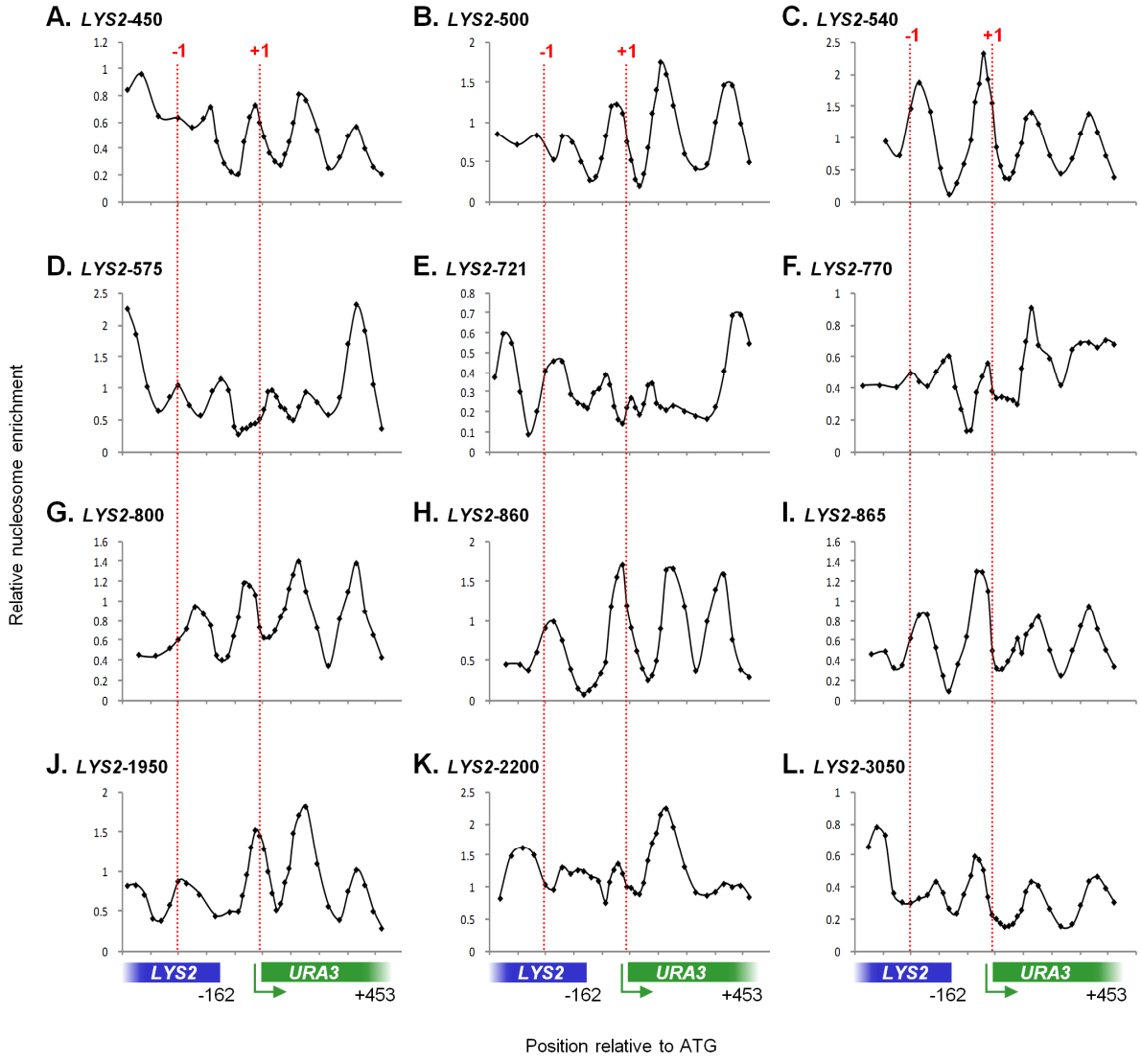

Figure S9. Nucleosome positions are influenced by the genomic context. Using tiling qPCR, we determined the nucleosome positions of the *URA3*-162 construct inserted at different positions in the *LYS2* gene. Peak positions corresponding to nucleosome positions were measured (Table SVI). Red dotted lines mark the positions of the -1 and +1 nucleosomes in the wild-type *URA3* promoter at its native locus.

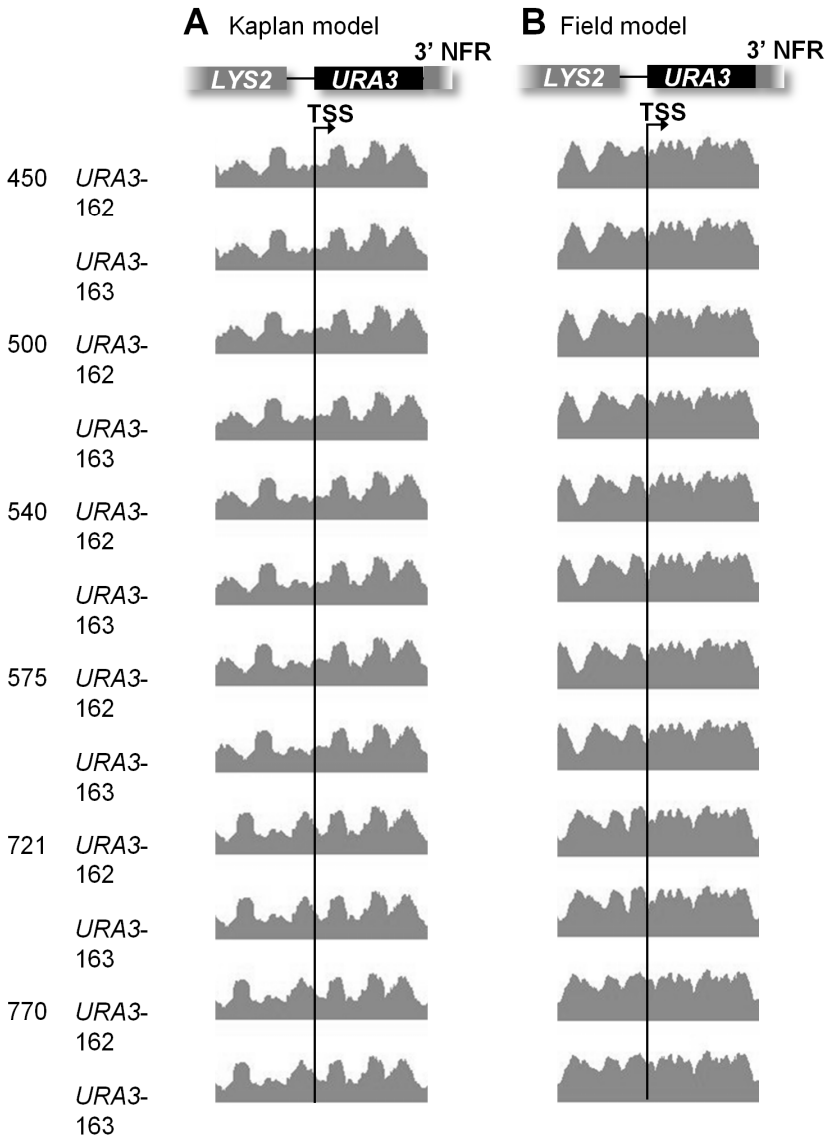

Figure S10. (figure legend on page S18)

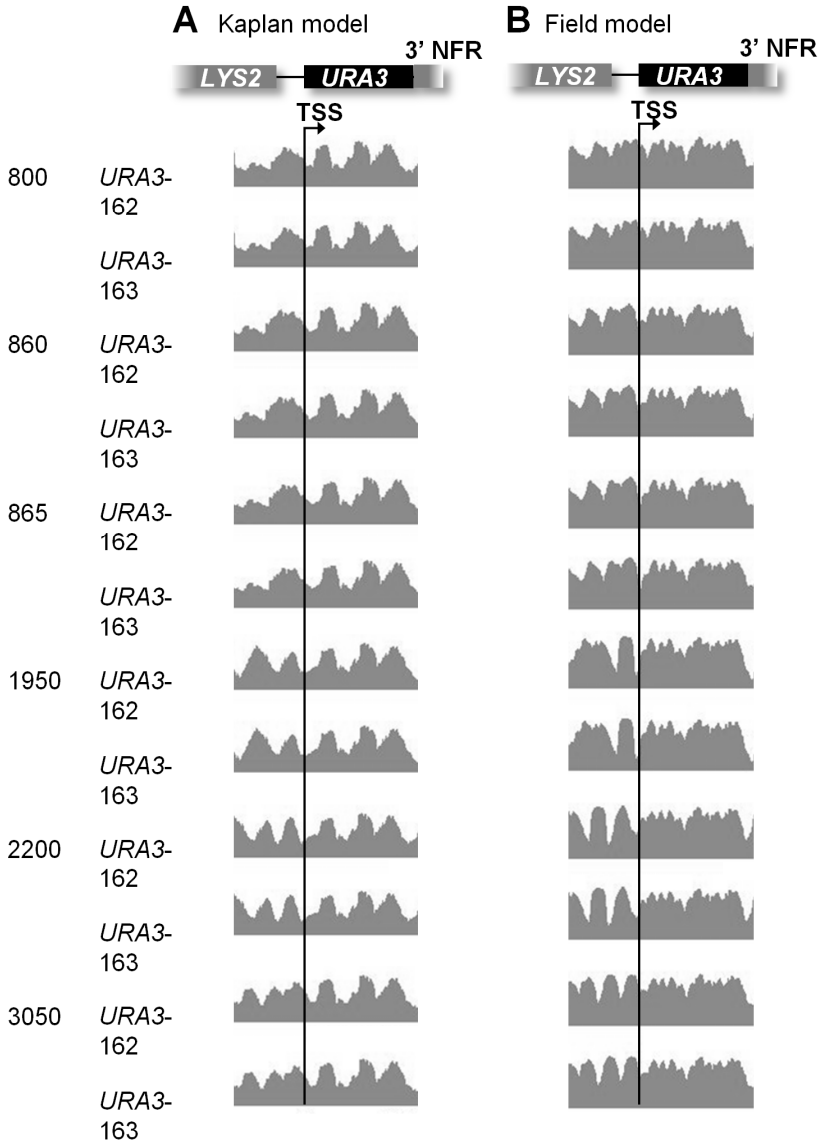

Figure S10 (continued from page S17). The predicted nucleosome positions of the *URA3*-162 and *URA3*-163 *lys2::URA3* mutants using (**A**) the Kaplan *et. al.* model (21) and (**B**) the Field *et. al.* model (15).

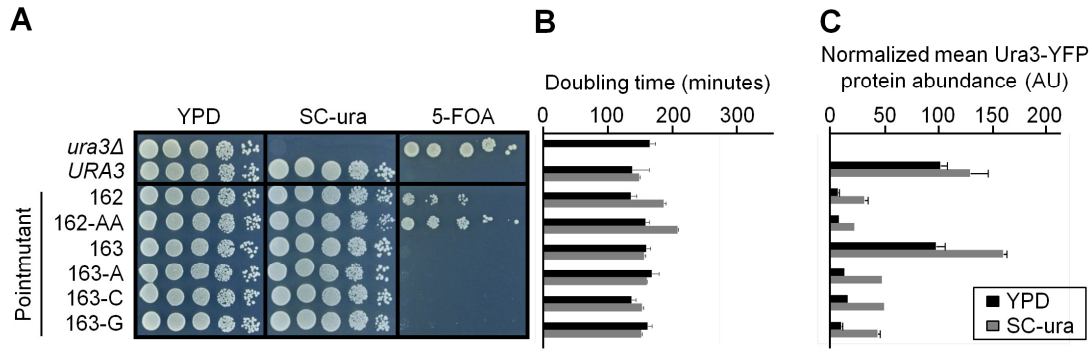

Figure S11. Characterization of the mutated *lys2::URA3* promoter strains. Mutants are labeled by their location inside the *LYS2* ORF, and by the pointmutation they contain. (**A**) Growth patterns on SC-ura and 5-FOA medium, (**B**) doubling times, and (**C**) normalized mean Ura3-YFP protein abundance for growth in liquid YPD (black bars) and liquid SC-ura (grey bars) media. Error bars denote standard deviation.

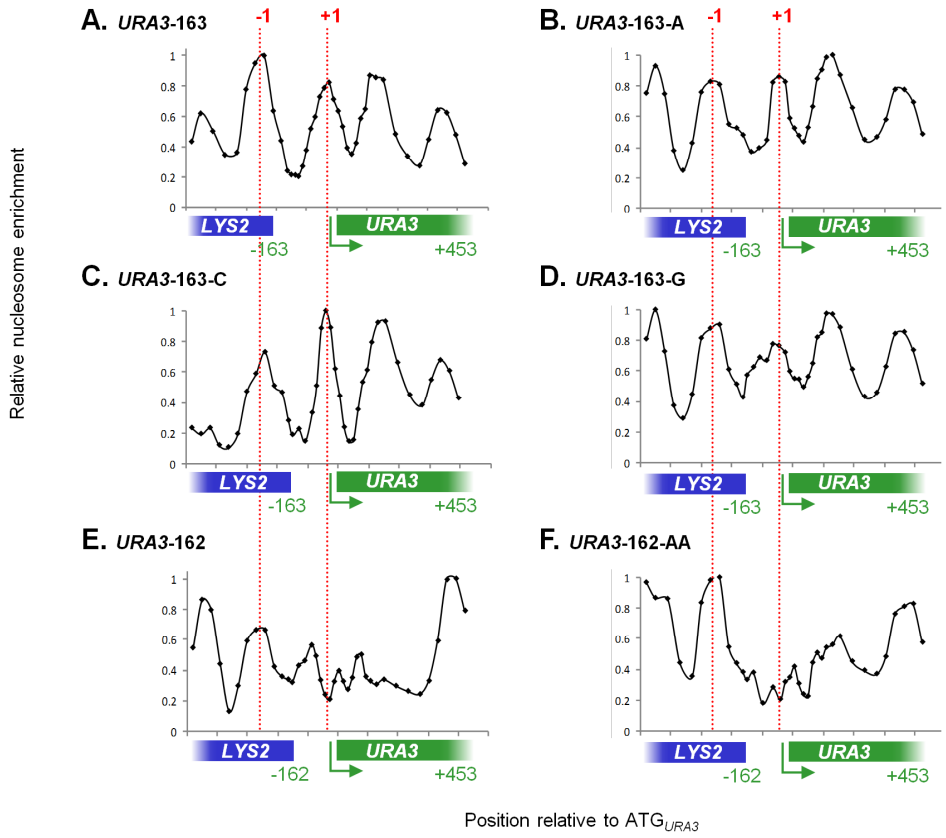

Figure S12. Nucleosome positions of the *URA3* promoter in the mutated *lys2::URA3* promoter strains. Using tiling qPCR, we determined the nucleosome positions of of the *URA3* promoter in strains (**A**) 163, (**B**) 163-A, (**C**) 163-C, (**D**) 163-G, (**E**) 162, and (**F**) 162-AA. Peak positions corresponding to nucleosome positions were measured (Table SVI). Red dotted lines mark the positions of the -1 and +1 nucleosomes in the wild-type *URA3* promoter at its native locus.

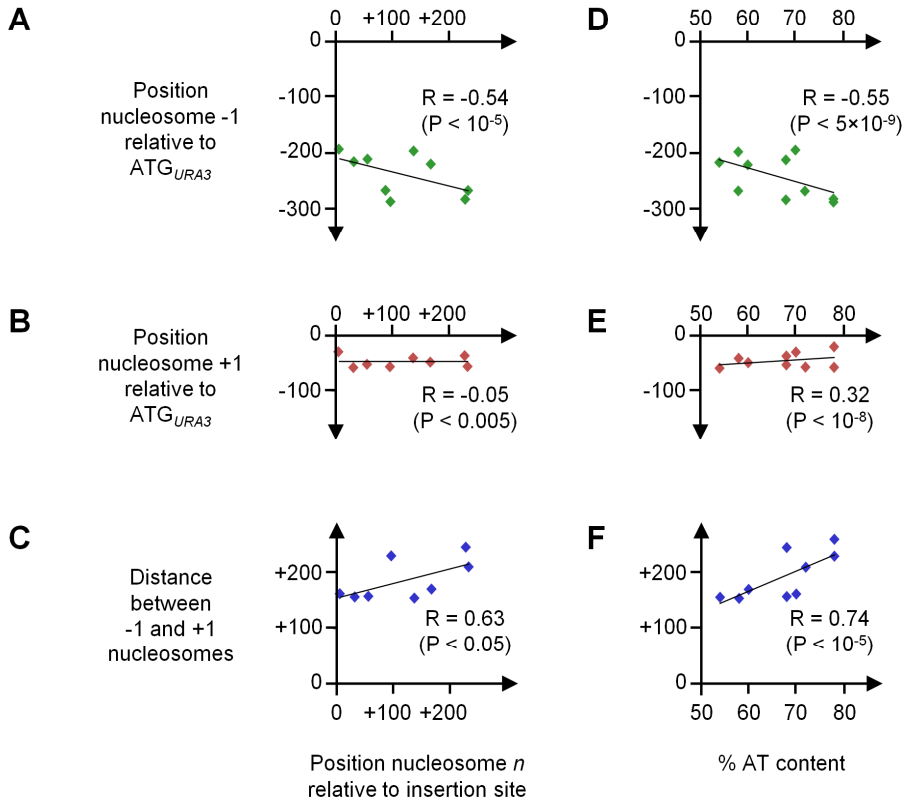

Figure S13. Genomic context influences the position of the -1 nucleosome but not the position of the +1 nucleosome of a truncated *URA3* promoter. The genomic context of each insertion site was quantified by measuring the position of the first nucleosome *n* upstream of each insertion site before insertion of the *URA3* gene (see Fig. 2B) and %AT content at the junction between the upstream *LYS2* sequence and the *URA3* promoter. The positions of the -1 nucleosome (**A**), the positions of +1 nucleosome (**B**) and the distance between the -1 and +1 nucleosomes (**C**) of the *URA3*-162 promoter after insertion into various locations of the *LYS2* gene are plotted against the position of nucleosome *n* before insertion. The positions of the -1 nucleosome (**D**), the positions of +1 nucleosome (**E**) and the distance between the -1 and +1 nucleosomes (**F**) of the *URA3*-162 promoter after insertion into various locations of the *LYS2* gene are plotted against %AT content at the junction between the upstream *LYS2* sequence and the *URA3* promoter. For each plot, the Pearson correlation coefficient was calculated.

Supplementary tables

Table SI. Strains.
Table SII. Plasmids.
Table SIII. Primers.
Table SIV. Sequences of tiling qPCR primers.
Table SV. Tiling qPCR primers for determining nucleosome positions.

Table SVI Positions of the *URA3* -1 and +1 nucleosomes

Insertion site[a]	Promoter length[b]	Position -1 nucleosome[c]	Position +1 nucleosome[c]	Distance[d]
LYS2-721	162	-266.41 +/- 5.22	noisy	n/a
LYS2-721, ΔP_{LYS2}	162	-274.96 +/- 4.31	noisy	n/a
LYS2-450	162	-192.47 +/- 0.97	-29.64 +/- 3.92	162.83 +/- 4.89
LYS2-500	162	-210.30 +/- 14.19	-52.02 +/- 2.58	158.28 +/- 16.77
LYS2-540	162	-286.71 +/- 19.59	-56.35 +/- 19.28	230.36 +/- 38.87
LYS2-575	162	noisy	noisy	n/a
LYS2-721	162	-266.41 +/- 5.22	noisy	n/a
LYS2-770	162	-195.69 +/- 18.31	-40.63 +/- 6.17	155.06 +/- 24.48
LYS2-800	162	-219.25 +/- 22.50	-48.14 +/- 6.64	171.10 +/- 29.14
LYS2-860	162	-282.49 +/- 7.16	-36.64 +/- 2.74	245.85 +/- 9.90
LYS2-865	162	-266.66 +/- 5.77	-55.95 +/- 2.57	210.72 +/- 8.33
LYS2-1950	162	-280.89 +/- 4.70	-20.34 +/- 1.38	260.55 +/- 6.08
LYS2-2200	162	noisy	noisy	n/a
LYS2-3050	162	-214.93 +/- 20.61	-57.83 +/- 7.91	157.09 +/- 28.53
LYS2-721	163	-259.29 +/- 2.26	-34.51 +/- 2.16	224.78 +/- 4.42
LYS2-721	163-A	-259.57 +/- 5.07	-47.55 +/- 2.81	212.02 +/- 7.88
LYS2-721	163-C	-242.88 +/- 3.57	-39.95 +/- 1.32	202.93 +/- 4.89
LYS2-721	163-G	-268.64 +/- 6.19	-71.62 +/- 5.72	197.02 +/- 11.91
LYS2-721	162	-266.41 +/- 5.22	noisy	n/a
LYS2-721	162-AA	-262.68 +/- 4.14	noisy	n/a

[a] Insertion site of the *URA3* reporter gene, at the native *URA3* locus ("native") or at the *LYS2* gene (e.g. "*LYS2*-721" indicates an insertion site is located 721 bp downstream of the *LYS2* START site).

[b] Length of the remaining truncated *URA*3 promoter (e.g. "162" indicates the promoter has the 162 bp most proximal to its START codon remaining). Δ*poly(dA:dT)* indicates the deletion of the poly(dA:dT) sequence only.

[c] Position of the nucleosome center relative to the *URA3* START site.

[d] Distance between the -1 and +1 nucleosome centers (see Fig. 2). The NFR width can be calculated by subtracting 147 bp from the distance.

Table SVII Positions of the *URA3* -1 and +1 nucleosomes

Insertion site[a]	Promoter length[b]	Growth medium[c]	Position -1 nucleosome[d]	Position +1 nucleosome[d]	Distance[e]
native	366	YPD	-303.12 +/- 2.5	-5.59 +/- 9.75	297.53 +/- 12.25
native	366	SC-ura	-302.61 +/- 19.48	0.16 +/- 3.1	302.77 +/- 22.58
LYS2-721	163	YPD	-259.29 +/- 2.26	-34.51 +/- 2.16	224.78 +/- 4.42
LYS2-721	163	SC-ura	-262.58 +/- 2.06	-35.52 +/- 2.22	227.06 +/- 4.28
LYS2-721	162	YPD	-266.41 +/- 5.22	noisy	n/a
LYS2-721	162	SC-ura	-268.52 +/- 3.38	noisy	n/a
LYS2-721	162	FOA	-277.34 +/- 4.41	noisy	n/a

[a] Insertion site of the *URA3* reporter gene, at the native *URA3* locus ("native") or at the *LYS2* gene (e.g. "*LYS2*-721" indicates an insertion site is located 721 bp downstream of the *LYS2* START site).

[b] Length of the remaining truncated *URA3* promoter (e.g. "162" indicates the promoter has the 162 bp most proximal to its START codon remaining). Δ*poly(dA:dT)* indicates the deletion of the poly(dA:dT) sequence only.

[c] Growth medium.

[d] Position of the nucleosome center relative to the *URA3* START site.

[e] Distance between the -1 and +1 nucleosome centers (see Fig. 2). The NFR width can be calculated by subtracting 147 bp from the distance.

Table SVIII Mutant *lys2::URA3* strains and their putative transcription factor binding sites. The displayed sequence is that of the junction between *LYS2* (in italics) and what remains of the *URA3* promoter. Point mutations are highlighted in bold. The UniPROBE database (56-58) was used to predict putative TF binding sites.

Strain	Sequence	TF	Putative TF binding site(s)
163	*GGGGTGTATTCAC*CTTTTTTGATTCGGTA	Sfp1	AC**T**TTTTT - C**T**TTTTTT - **T**TTTTTTG
		Sum1	**T**TTTTTTG
163-A	*GGGGTGTATTCAC***A**TTTTTTGATTCGGTA	none	
163-C	*GGGGTGTATTCAC***C**TTTTTTGATTCGGTA	none	
163-G	*GGGGTGTATTCAC***G**TTTTTTGATTCGGTA	Cbf1	TCAC**G**TTT
		Pho4	CAC**G**TTTT
162	*GGGGTGTATTCAC*TTTTTTGATTCGGTA	Sfp1	ACTTTTTT
162-AA	*GGGGTGTATTCAC***AA**TTTTGATTCGGTA	*Matalpha2**	*TCAC**AA**TT - CAC**AA**TTT - AC**AA**TTTT*

* Our studies were performed in *MATa* cells

Supplementary references

47. Ausubel, F.M. (1987) *Current protocols in molecular biology*. Published by Greene Pub. Associates and Wiley-Interscience : J. Wiley, New York.

48. Gietz, R.D., Schiestl, R.H., Willems, A.R. and Woods, R.A. (1995) Studies on the transformation of intact yeast cells by the LiAc/SS-DNA/PEG procedure. *Yeast*, **11**, 355-360.

49. Sherman, F., Fink, G.R. and Hicks, J. (1991) *Methods in yeast genetics*. Cold Spring Harbor Laboratory Press, Cold Spring Harbor, N.Y.

50. Storici, F., Lewis, L.K. and Resnick, M.A. (2001) In vivo site-directed mutagenesis using oligonucleotides. *Nat Biotechnol*, **19**, 773-776.

51. Chattoo, B.B., Sherman, F., Azubalis, D.A., Fjellstedt, T.A., Mehnert, D. and Ogur, M. (1979) Selection of lys2 Mutants of the Yeast SACCHAROMYCES CEREVISIAE by the Utilization of alpha-AMINOADIPATE. *Genetics*, **93**, 51-65.

52. Zaret, K.S. and Sherman, F. (1985) alpha-Aminoadipate as a primary nitrogen source for Saccharomyces cerevisiae mutants. *J Bacteriol*, **162**, 579-583.

53. Sheff, M.A. and Thorn, K.S. (2004) Optimized cassettes for fluorescent protein tagging in Saccharomyces cerevisiae. *Yeast*, **21**, 661-670.

54. Pernambuco, M.B., Winderickx, J., Crauwels, M., Griffioen, G., Mager, W.H. and Thevelein, J.M. (1996) Glucose-triggered signalling in Saccharomyces cerevisiae: different requirements for sugar phosphorylation between cells grown on glucose and those grown on non-fermentable carbon sources. *Microbiology*, **142**, 1775-1782.

55. Sambrook, J., Fritsch, E.F. and Maniatis, T. (1989) *Molecular Cloning: A Laboratory Manual*. 2 ed. Cold Spring Harbor Laboratory Press, Plainview, NY.

56. Blosser, T.R., Yang, J.G., Stone, M.D., Narlikar, G.J. and Zhuang, X. (2009) Dynamics of nucleosome remodelling by individual ACF complexes. *Nature*, **462**, 1022-1027.

57. Berger, M.F., Philippakis, A.A., Qureshi, A.M., He, F.S., Estep, P.W., 3rd and Bulyk, M.L. (2006) Compact, universal DNA microarrays to comprehensively determine transcription-factor binding site specificities. *Nat Biotechnol*, **24**, 1429-1435.

58. Zhu, C., Byers, K.J., McCord, R.P., Shi, Z., Berger, M.F., Newburger, D.E., Saulrieta, K., Smith, Z., Shah, M.V., Radhakrishnan, M. *et al.* (2009) High-resolution DNA-binding specificity analysis of yeast transcription factors. *Genome Res*, **19**, 556-566.